論 文 の 内 容 の 要 旨

論文題目　Functionalized nanoparticles for sensing and separation of biomolecules
（機能性ナノ粒子の生体分子検出・分離への応用）

氏　名　卜 同

1 Introduction

Nanoparticle (NP) refers to ultrafine particle with a dimension ranging from 1 to 100 nm. The small size of NPs results in quantum confinement effects and consequently in the tunable optical and electronic properties by changing the size, shape, surface chemistry, or aggregation state. These special physical properties of NPs opens up numerous research directions for medicine and life sciences, includes the use of NPs in drug delivery, cell imaging, and the NP-assisted gene therapy, just to name a few.

However, while some of the nanomaterial-based technologies have been applied to clinical settings; many nanotechnologies are still under experimental stage due to various drawbacks such as low detection sensitivity, lack of specificity, *et al.* In my study, application-oriented study of functional NP was explored in a way to reach a biomedical design target. Microscopic method was employed to improve the sensitivity of gold nanoparticle (AuNP)-based DNA mutation detection; antibody-conjugated AuNPs was designed and synthesized for the detection of amyloid protein aggregation. Furthermore, a ferromagnetic NP was used in the selective clearance of amyloid aggregates from monomers.

2 Detection of DNA induced gold nanoparticle aggregation with dark field imaging

Among various metal particles, AuNPs have attracted attention due to their advantageous properties involving stability, activity, conductivity, and surface chemistry. In particular, assemblies of AuNPs provide optical and electrical properties that are distinct from individual particles. For example, aggregation of AuNPs accompanied by the surface plasmon shift can be recognized by a clear color change (from red to purple), which enables potential applications in sensors for DNA, heavy metal ions and proteins[1]. In this study, single molecule approach using dark field microscopy (DFM) was applied to examine AuNPs aggregation allowing the highly sensitive detection possible.

The single-stranded probe DNA was immobilized on the surface of AuNPs through Au-S bond formation (ssDNA-AuNPs). Various amounts of complementary ssDNA were added into the ssDNA-AuNPs dispersion solution in the presence of 1 M NaCl. For the DFM analysis, the AuNPs samples were deposited onto glass-slides. DFM images were taken using microscope equipped with dark field condenser, and the size of

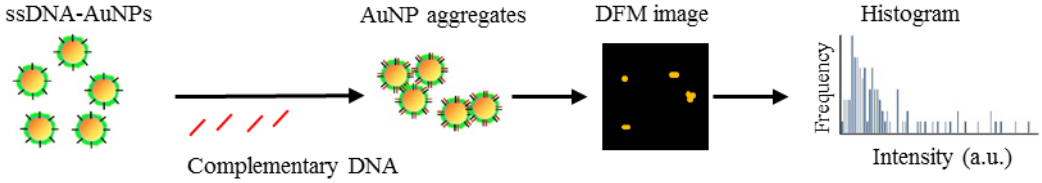

Fig. 1 Schematic diagram illustrating procedures of detection of complementary DNA induced AuNP aggregation by DFM

AuNPs aggregates was estimated by the intensity of each spot in DFM images. The change in the intensity histograms was used to determine the limit of detection (LOD) of the target ssDNA by 3σ criterion method and to investigate AuNPs aggregation models.

As shown in Fig. 2a, the dispersed (left) and aggregated AuNPs (right) were identified in DFM images as spots. Figure 2b shows intensity histograms of dispersed and aggregated AuNPs induced by addition of various amounts of target ssDNA, which indicate the size and number of each AuNPs aggregation. As shown in Fig. 2c, the addition of increasing concentrations of target ssDNA into the ssDNA-AuNP solution resulted in particles with higher intensities. The LOD was determined as low as 100 fM.

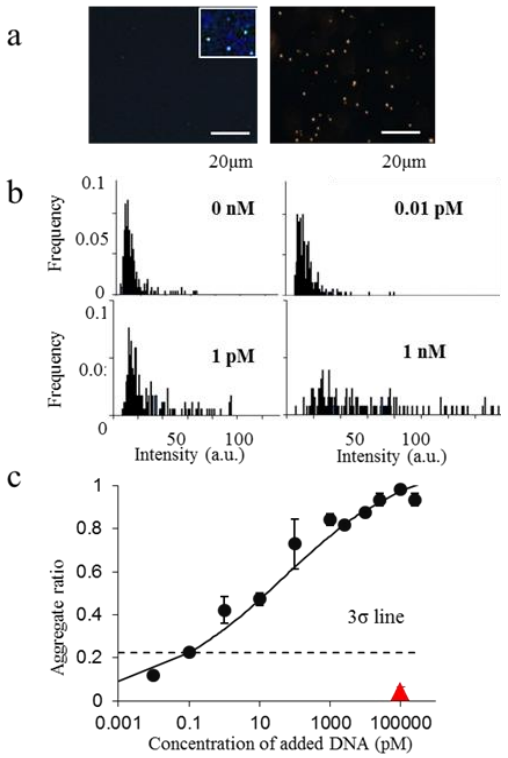

Fig.2 (a)DFM images of dispersed and aggregated AuNPs, (b)Intensity histogram of AuNPs aggregates observed by DFM (c)Determination of LOD

Taking advantage of single-particle level measurement, the dsDNA-AuNP aggregation model was investigated by studying the assembly dynamics using DFM. The two NPs aggregate growth models, namely, particle-cluster and cluster-cluster models, were proposed based on modelling of theoretical phenomena and computer simulations (Fig.3a)[2]. Although it was difficult to confirm the hypothesis experimentally due to the heterogeneity of NPs aggregates, this problem can be overcome by studying the aggregate at single-cluster level. First, the aggregation time scale was roughly estimated by DLS (Fig.3b, open triangle). The size of aggregation indicates that the aggregation process is still in progress after 2 hours of incubation. The change of the ratio of monomer AuNPs over time after the addition of 50 nM of target ssDNA was then estimated with DFM as described above (Fig. 3b closed circle). The result indicates that monomer-cluster aggregation model is unlikely to account for our results, indirectly suggesting that cluster-cluster aggregation is the dominant model for dsDNA-AuNP aggregation at the early stage.

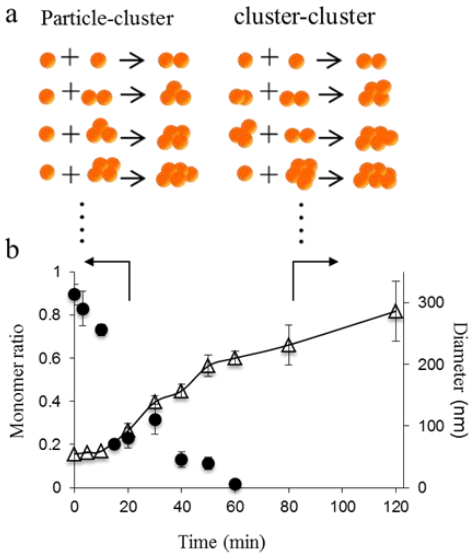

Fig. 3 (a) Schematic diagram of NPs aggregation models (b) DNA induced AuNPs aggregation

In conclusion, we have demonstrated for the first time that DFM can be utilized for the highly sensitive detection of DNA induced AuNPs aggregation at the single-cluster level. The sensitivity was much better than that obtained with conventional methods such as color change, UV-Vis spectroscopy and DLS. Our DFM results also suggest that the aggregation process at the early stage follows the cluster-cluster aggregation model. These capabilities should open opportunities for the use of DFM in various analytical methods using NPs assembly.

3 Dark field microscopic detection of amyloid aggregates using gold nanoparticles modified with antibody

The amyloid beta (Aβ) protein is a 39- to 43-amino acid polypeptide that is the primary constituent of senile

plaques and cerebrovascular deposits in Alzheimer's disease (AD)[3]. The formation of Aβ aggregates is considered to cause AD neuro-degeneration by affecting brain nerve cells. Therefore, detection of Aβ aggregates is important for early recognition of diseases. Previous study reported that amyloid aggregates can be detected by the precipitation of AuNPs conjugated with Aβ antibodies (Ab)[4]. Red-colored precipitates can be seen by naked-eye by addition of 5 μM Aβ aggregates into AuNP-antibody (Ab-AuNP) colloid. However, this detection method is not sensitive enough for practical clinical use. In an aim to achieve higher sensitivity of Aβ aggregates detection, DFM was utilized to detect the Aβ aggregates-induced AuNPs assembly.

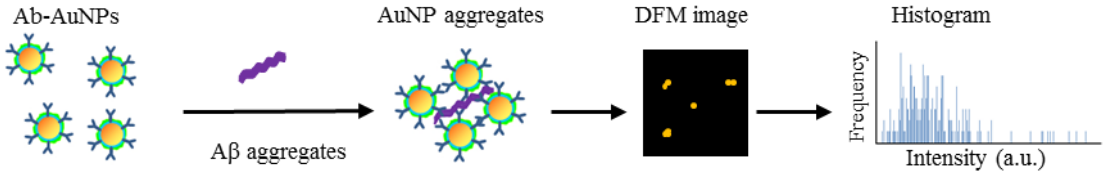

Fig.4 Schematic diagram illustrating the procedures of DFM detection of Abeta aggregates using AuNP-antibody

Aβ fibril was prepared as previously described with some modification[5]. Anti-Aβ antibody was immobilized onto the negatively charged AuNPs surface as reported[4]. The Ab-AuNPs were treated with bovine serum albumin (BSA) for dispersibility in buffer. The prepared Ab-AuNP were mixed with Aβ monomer, and fibril solution at certain concentrations, and incubated at room temperature for 1 h. The absorbance and size change of AuNPs were determined by UV-Vis spectroscopy and DLS, respectively. DFM images of AuNPs samples were taken as described above.

After addition of Aβ monomer and fibril at the same concentration, there was no color change distinguishable by naked eye and there was no peak-shift in the result of UV-vis spectroscopy (Fig. 5a and b). However, as shown in Fig. 5c, mixture of Ab-AuNP with fibril sample showed much brighter spots in DFM images than Ab-AuNP sample with addition of monomer. The addition of increasing concentrations of target Aβ oligomer/fibril into the Ab-AuNP solution resulted in particles with higher intensities. Similar to the method stated above, the LOD was determined as 7 pM for oligomer and 39 pM for fibril detection.

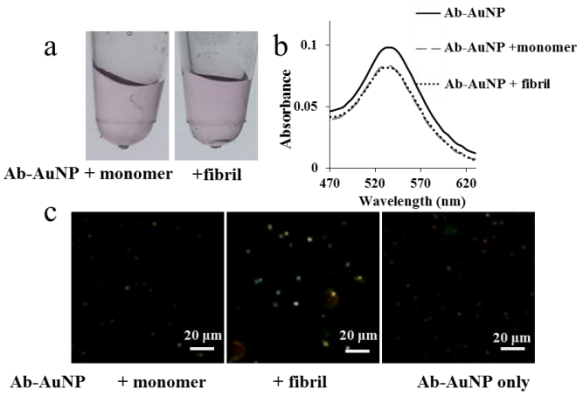

Fig. 5 Aβ monomer and fibril interaction with AuNP with antibody immobilized on the surface. (a) Color change; (b) UV-Vis spectroscopy; (c) DFM images

4 Magnetic nanoparticles for selective amyloid aggregates adsorption and separation

As stated above, both oligomeric and fibrillar Aβ aggregates are targets for therapy design in AD. Interaction between nano-materials and Aβ protein has attracted increasing attention. In this chapter, we explored the use of NPs in distinguishing and separating selectively the aggregates from monomers.

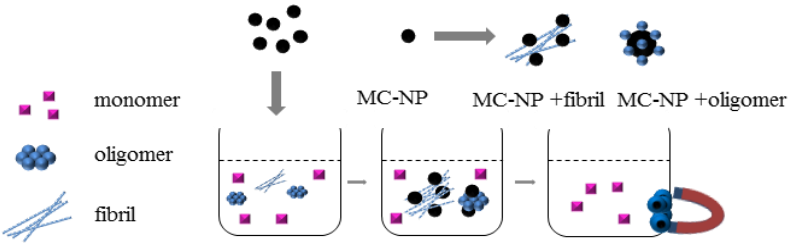

Fig. 6 Schematic diagram illustrating the procedures of selective Abeta aggregates adsorption on MC-NPs

Ferromagnetic NPs PolyMAPTAC (poly[3-(methacryloyl amino)propyl] trimethylammonium chloride) Co/C (MC-NP) was employed. The selective binding and separation of aggregates using MC-NPs was confirmed by dot blot (monomer and fibril) and Western Blot (oligomer).

As shown in Fig. 7a, when 12.5 μM of Aβ monomer and fibrils were incubated with 50 μg/mL MC-NPs for 1 h, no fibril was left in the supernatant, while no significant change of the amount of monomer in the supernatant observed. When MC-NPs were added into the mixture of oligomer and monomers, oligomer was clearly removed, and monomers were left without absorbing to MC-NPs (Fig. 7b). These results indicate that MC-NPs could selectively bind to Aβ fibrils and oligomers. Interaction between MC-NPs and fibrils and oligomers was confirmed by TEM observation (Fig. 7c). The study of adsorption kinetics showed that the adsorption of fibrils onto NPs surface is a rapid process. The adsorption capacity of Aβ fibril by MC-NPs was determined as 1:2 (weight) after 1 h incubation (Fig. 8). This result implies potential application of MC-NPs in the diagnosis and treatment of various diseases related to amyloid aggregates.

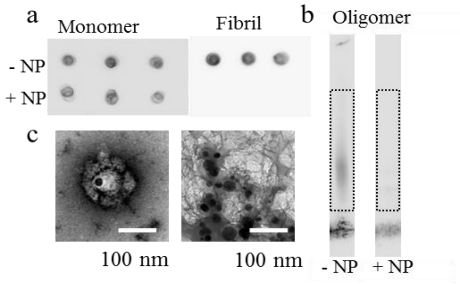

Fig. 7 Interaction between Aβ protein and MC-NPs. (a) dot blot; (b) WB; (c) TEM images

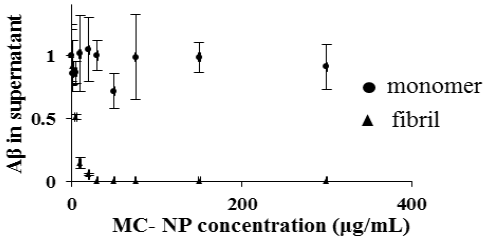

Fig. 8 Characterization of adsorption of monomer and fibrils on MC-NP

5 Conclusion and perspectives

In this study, the potential of NP in biomedical applications have been explored: SNPs in DNA can be detected using AuNPs with high sensitivity; Aβ aggregates that related to AD can not only be early sensed using antibody immobilized AuNPs, but also be clarified by magnetic MC-NP in solution. Successful development in these studies will aid the growth of biomedical industry as well as improving the quality of life in the population.

Reference:

1. (a) Mirkin, C. A.; Letsinger, R. L.; Mucic, R. C.; Storhoff, J. J.,. *Nature* **1996,** *382*, 607-609; (b) Sato, K.; Hosokawa, K.; Maeda, M., *J. Am. Chem. Soc.* **2003,** *125* (27), 8102-8103.

2. Hemker, D. J.; Frank, C. W., *Macromolecules* **1990,** *23* (20), 4404-4410.

3. Yankner, B. A.; Duffy, L. K.; Kirschner, D. A., *Science* **1990,** *250* (4978), 279-282.

4. Sakono, M.; Zako, T.; Maeda, M., *Anal. Sci.* **2011,** *28* (1), 73-73.

5. Kayed, R.; Head, E.; Sarsoza, F.; Saing, T.; Cotman, C. W.; Necula, M.; Margol, L.; Wu, J.; Breydo, L.; Thompson, J. L., *Mol Neurodegener* **2007,** *2* (18), 18.